SIMULATION OF THE AIRCRAFT CABIN COOL-DOWN AND WARM-UP PROCESSES

Edson Luiz Zaparoli
zaparoli@mec.ita.br
Cláudia Regina de Andrade
claudia@mec.ita.br

Instituto Tecnológico de Aeronáutica – Departamento de Energia.
Pça Marechal Eduardo Gomes, 50 – Vila das Acácias.
12228-900 – São José dos Campos, SP, Brasil.

Abstract. *The main design requirements of the aircraft environmental control system are the cabin cooling-heating loads and the cool-down and warm-up time periods. The cool-down process is the cooling of a heat-soaked aircraft prior to passenger loading and the warm-up process is the heating of a cold-soaked empty aircraft cabin. In this study the aircraft cabin cool-down and warm-up processes are mathematically modeled and numerically solved to study the influence of the air conditioning machine parameters and the cabin external and internal characteristics. The mathematical model couples the lumped parameters method with a differential approach to reduce the computational effort to solve this problem. This computational tool will reduce both the spent design time and the number of experimental tests to adjust the final environmental control system configuration.*

Keywords*. cool-down, warm-up, ecs, aircraft air-conditioning.*

1. Introduction

This study deals with the numerical simulation of transient thermal process in a typical aircraft cabin. Temperature, humidity, pressure and air velocity must be kept at a given range with an Environmental Control System (ECS) to provide a suitable thermal control for the avionics and to satisfy the people thermal comfort requirements. To design an aircraft ECS is very important to calculate its steady-state and transient performance. The cool-down process is the cooling of a heat-soaked aircraft prior to passenger loading and the warm-up process corresponds to the heating of a cold-soaked empty aircraft cabin. Both cool-down and warm-up time intervals of less than 30 minutes are usually specified. The sizing criteria for the air conditioning may be the steady-state operation on a hot, humid day with the aircraft fully loaded and the doors closed or the cool-down/warm-up transient performance. To simulate these two transient processes, the cabin heating and cooling thermal loads at ground conditions must be evaluated.

Many studies have focused on the simulation of the heat transfer process of passengers' compartment. Conceição et al. (1999) developed a computational model with the objective of simulating the thermal behavior of the passengers' compartment of vehicles. Their model is based on the lumped capacitance energy balance equations for the air inside the compartment and for the main vehicle bodies and surfaces. The numeric simulation showed a good agreement with available experimental results.

Ding and Zito (2001) considered an automotive vehicle's cabin and applied the lumped capacitance method to establish a relationship between interior temperature changes vs. time during a typical cool-down or idle test. The proposed methodology also determines an overall heat transfer coefficient that becomes a link between the demand from the air side and the supply from the refrigerant-side. Their work provides a tool in aiding the design of an air conditioning system based on the consumer comfort.

An interior comfort engineering computer-aided engineering tool was developed by Gielda et al. (1996) to allow the design of automotive climate control systems in which passenger thermal comfort was the primary performance benchmark. Their computational code was based on the finite element technique solving the incompressible thermally coupled Navier-Stokes equations. The extremely intensive calculations were performed on parallel architecture computers and the results included simulations of both winter warm-up and summer pull-down testing. In addition, results from solar soak precondition simulations were presented and compared with existing climate control wind tunnel test data.

Fang (1999) developed a mathematical model to calculate the temperature time evolution of the floors, partitions, windshields, covers and skin of an aircraft cabin. This author employs the finite difference method to solve the equations system of the mathematical model. The author attacks two kinds of problems. In the first one, calculates the heat stress that the air conditioning or heating system must balance, in order to satisfy predefined steady state project specifications. In the second one, once imposed a particular air conditioning system and given the ambient conditions, it computes the different temperatures and heat fluxes either in transient or steady regimens. The proposed model reproduced well the experimentally determined temperature and heat fluxes evolutions.

In the present study, the unsteady temperature of a typical aircraft cabin cross-section is simulated applying the lumped parameters approach. The interrelated cabin thermal components (sub-domains) temperatures are modeled by a time-dependent ordinary differential equations system which is numerically solved using a fourth-order Runge-Kutta scheme. Both warm-up and cool-down results obtained with this mathematical simulation provides a useful tool to support the design of the cabin aircraft environmental control system.

2. Mathematical Formulation

Figure (1) presents a typical lengthwise cabin ventilation pattern that is designed to avoid the aerosols contaminants longitudinal transport due to the airflow trough the passenger high density cabin. By design considerations, the cabin lengthwise air inflow is equal to the outflow quantity to avoid the mentioned longitudinal flow. This flow pattern allows a simplified thermal model for a cabin finite element including a single cross-section seat row.

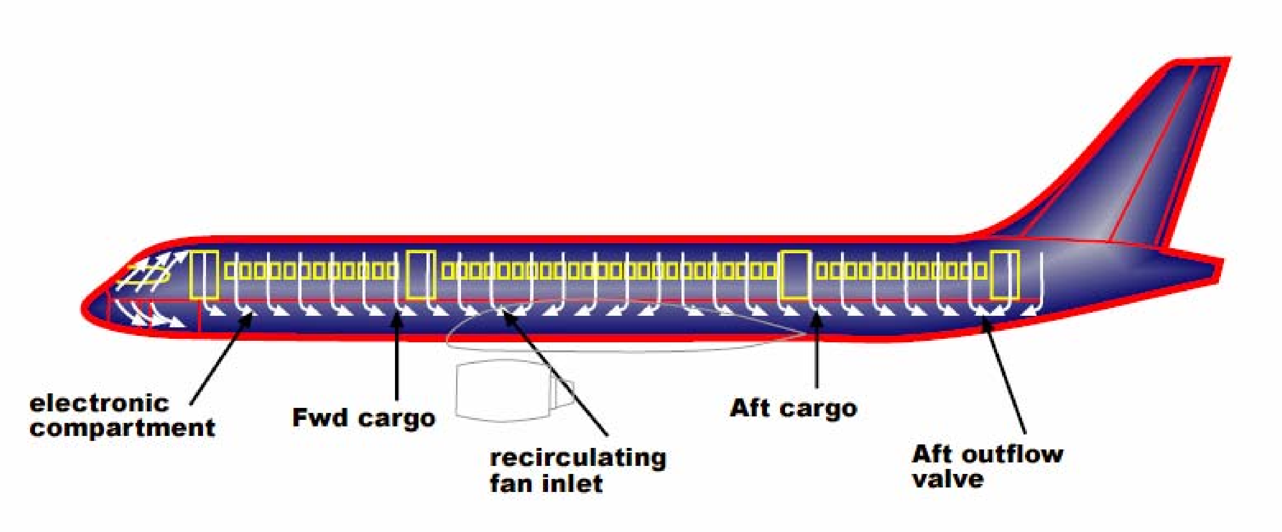

Figure 1. Lengthwise cabin ventilation pattern.

The desired cabin cross-section airflow is presented in Fig. (2), which results in a well-mixed air condition due to the intense mixing process. Under these conditions it is suitable to apply the lumped parameter method to model the time-dependent uniform air temperature. This temperature is one ambient factor related to the passenger thermal comfort.

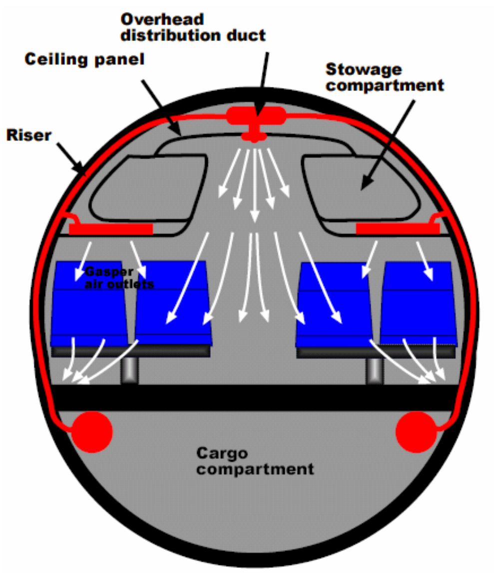

Figure 2. Cabin cross-section airflow ventilation pattern.

In this study the lumped parameters method is employed assuming that the Biot numbers associated with conduction heat transfer in each cabin solid sub-domains are far less than unity (Fig. 2). This method can still be used for the cabin inside air as long as the interior temperature is within a fairly degree of uniformity which is achieved by mixing effects of forced convection from the blower with interior air. Even when the above conditions aren't fully satisfied, a simple and easy computational model often used in the ECS control system design is obtained with this approach (Conceição et al., 1999; Ding and Zito, 2001; Kasahara et al., 1998; Huang et al., 1999; Kojima et al., 1999).

The unsteady heat transfer process for each cabin sub-domain is shown in Fig. (3). The one-dimensional thermal resistance concept is used to represent the heat transfer mechanism between each cabin sub-domain pair.

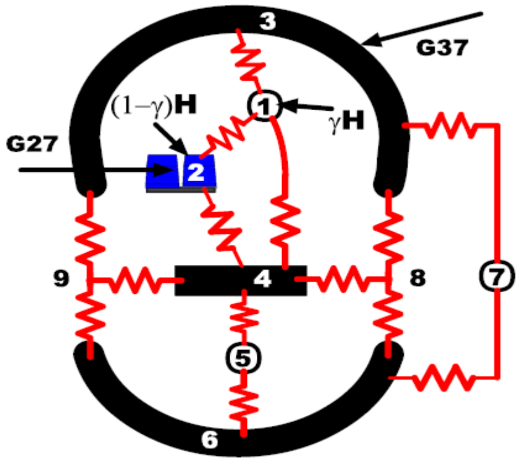

Figure 3. Cabin cross-section thermal model: lumped parameter and one-dimensional thermal resistance.

Table (1) shows the cabin sub-domains nomenclature, description and heat transfer interactions. Labels 7, 8 and 9 refer to the nodes in the analog thermal resistance model and represent the outside ambient air, the right and left joints among upper fuselage wall, floor and lower fuselage wall, illustrated in Fig. (3).

Table 1. Cabin sub-domains.

Cabin sub-domains	Description	Heat exchange with
1	Cabin inside air	[2,3,4]
2	Seat	[1,4]
3	Upper fuselage wall	[1,7,8,9]
4	Floor	[1,2,5,8,9]
5	Under floor air	[4,6]
6	Lower fuselage wall	[5,7,8,9]

The energy balance for each cabin cross-section sub-domain results in the following ordinary differential equation system:

$$m_1 Cp_1 \frac{dT_1}{dt} = N\, U_{12} A_{12}\,(T_2 - T_1) + U_{13} A_{13}\,(T_3 - T_1) + U_{14} A_{14}\,(T_4 - T_1) + \dot{m}_{in1} Cp_1 (T_{in1} - T_1) + E_1 + N\,(\gamma H) \tag{1}$$

$$m_2 Cp_2 \frac{dT_2}{dt} = U_{12} A_{12}\,(T_1 - T_2) + U_{24} A_{24}\,(T_4 - T_2) + (\alpha_2 G_{27}) A_{27} + (1 - \gamma)\, H \tag{2}$$

$$m_3 Cp_3 \frac{dT_3}{dt} = U_{13} A_{13}\,(T_1 - T_3) + U_{37} A_{37}\,(T_7 - T_3) + U_{38} A_{38}\,(T_8 - T_3) + U_{39} A_{39}\,(T_9 - T_3) + (\alpha_3 G_{37})(\beta A_{37}) \tag{3}$$

$$m_4 Cp_4 \frac{dT_4}{dt} = U_{14} A_{14}\,(T_1 - T_4) + N U_{24} A_{24}\,(T_2 - T_4) + U_{45} A_{45}\,(T_5 - T_4) \quad U_{48} A_{48}\,(T_8 - T_4) + U_{49} A_{49}\,(T_9 - T_4) \tag{4}$$

$$m_5 Cp_5 \frac{dT_5}{dt} = U_{45}A_{45}\,(T_4 - T_5) + U_{56}A_{56}\,(T_6 - T_5) + \dot{m}_{in5} Cp_5 (T_1 \;\; - T_5) + E_5 \tag{5}$$

$$m_6 Cp_6 \frac{dT_6}{dt} = U_{56}A_{56}\,(T_5 - T_6) + U_{67}A_{67}\,(T_7 - T_6) + U_{68}A_{68}\,(T_8 - T_6) \tag{6}$$
$$U_{69}A_{69}\,(T_9 - T_6)\; + (\alpha_6 G_{67})A_{67}$$

$$T_8 = T_9 \tag{7}$$

$$T_9 = \frac{U_{39}A_{39}T_3 + U_{49}A_{49}T_4 + U_{69}A_{69}T_6}{U_{39}A_{39} + U_{49}A_{49} + U_{69}A_{69}} \tag{8}$$

$$\dot{m}_{in1} = \dot{m}_{out1} = \dot{m}_{in5} = \dot{m}_{out5} \tag{9}$$

Where:

T_i	analog thermal circuit node temperature;
m_i	cabin sub-domain mass;
Cp_i	cabin sub-domain constant pressure specific heat;
$U_{ij}= U_{ji}$	heat transfer global coefficient between i node and j node of the analog thermal circuit;
$A_{ij}= A_{ji}$	heat transfer area between i node and j node of the analog thermal circuit;
N	passenger number in each cabin cross-section seat row;
H	sensible heat dissipated by each passenger;
$\dot{m}_{in1} = \dot{m}_{in5}$	input mass flow rate to the cabin and under floor compartments;
T_{in1}	input cabin air temperature;
E_1	electrical energy dissipated inside the cabin;
E_5	electrical energy dissipated inside the under floor compartment;
G_{i7}	direct solar irradiation to the i sub-domain;
α_i	i sub-domain absorptivity;
$\beta = 2/\pi$	ratio of the projected area of the fuselage to the total area;
γ	fraction of passenger sensible heat exchanged with the cabin air.

Temperature of nodes 8 and 9 were determined by performing a steady-state energy balance (Eqs. 7 and 8).

3. Solution Methodology

In the present study the lumped parameter method was employed to simulate the cabin aircraft thermal behaviour. As a result, a set of time-dependent ordinary differential equations (ODE) was obtained (Eq. 1 to Eq. 6) associated with each cabin sub-domain. These equations were numerically solved using a fourth-order Runge-Kutta scheme (Hoffman, 1993). This method allows higher-order accuracy by introducing intermediate integration points between points *n* and *n+1*.

The basic idea of Runge-Kutta methods is to consider that $\Delta y_n = y_{n+1} - y_n$ is the weighted summation of several Δy_i (i = 1, 2, …), where each Δy_i is based on several values of the derivative function f (t, y) evaluated at different arguments. Thus, it can be written that:

$$y_{n+1} - y_n = C_1 \cdot \Delta t \cdot f(t_n, y_n) + C_2 \cdot \Delta t \cdot f(t_n + \alpha_2, y_n + \beta_2) + C_3 \cdot \Delta t \cdot f(t_n + \alpha_3, y_n + \beta_3) + \dots \tag{10}$$

where the free parameters C1, C2, α_2, α_3, β_2, β_3, …, are chosen by requiring that Eq. (7) to match the Taylor series for the exact solution through terms of a specific order. The most popular Runge-Kutta scheme is the fourth-order method here used, as follow:

$$y_{n+1} = y_n + \frac{1}{6}\left(\Delta y_1 + 2\Delta y_2 + 2\Delta y_3 + \Delta y_4\right) \tag{11}$$

with: $\Delta y_1 = \Delta t \cdot f[t_n, y_n]$; $\Delta y_2 = \Delta t \cdot f\left[\left(t_n + \frac{\Delta t}{2}\right), \left(y_n + \frac{\Delta y_1}{2}\right)\right]$; $\Delta y_3 = \Delta t \cdot f\left[\left(t_n + \frac{\Delta t}{2}\right), \left(y_n + \frac{\Delta y_2}{2}\right)\right]$ and

$$\Delta y_4 = \Delta t \cdot f\,[(t_n + \Delta t),(y_n + \Delta y_3)\,]$$

This scheme requires four derivative function evaluations per step. Besides, the local single-step gives a truncation error of order Δt^5 and the global error is $O\ (\Delta t^4)$.

4. Results

In the present study, the cabin input $(\dot{m}_{in1})$ and output $(\dot{m}_{out1})$ mass flow rates are equal. This is also the same air flow rate supplied to the under-floor compartment $(\dot{m}_{in5})$. For both warm-up and cool-down processes, the cabin pressure is assumed constant and there are four passengers in each seat row of the cabin cross-section (N = 4 in Fig. 2). The certification requirements (ASHRAE, 1999) impose a minimum input volumetric air-flow rate of 10 liters/s (or 0.012 kg/s) per passenger.

The warm-up or cool-down processes take place at ground conditions before passenger entrance with no electrical energy dissipating, implying that H = 0, $E_1 = 0$ and $E_5 = 0$. Results presented in this study are γ-independent because H = 0.

A hypothetical aircraft with typical geometric dimensions (obtained from details drawings) and materials properties is assumed to calculate the one-dimensional heat flow rate. Values for mass and constant pressure specific heat related to each cabin sub-domain are shown in Tab. (2).

Table 2. Cabin sub-domains material properties.

Sub-domain	m [kg]	Cp [J/kg·K]
Cabin inside air	1.2	1007.0
Seat	6.0	1100.0
Upper fuselage wall	50	875.0
Floor	50	900.0
Under floor air	0.4	1007.0
Lower fuselage wall	40.0	875.0

To evaluate the overall heat transfer coefficients, a simplified steady-state one-dimensional heat transfer analysis is employed along the heat flow paths presented in Fig. (3). Table (3) shows the results for the heat transfer areas and the global heat transfer coefficients obtained by taking account the equivalent thermal circuit for each heat flow path.

Table 3. Global heat transfer coefficients and heat exchange areas values.

U_{ij}	Value [W/m^2·K]	A_{ij}	Value [m^2]
U_{12}	4.0	A_{12}	1.0
U_{13}	3.0	A_{13}	3.0
U_{14}	2.0	A_{14}	2.0
U_{24}	0.5	A_{24}	0.05
U_{37}	50.0	A_{37}	2.0
U_{38}	1.5	A_{38}	0.1
U_{39}	1.5	A_{39}	0.1
U_{45}	4.0	A_{45}	2.0
U_{48}	1.5	A_{48}	0.1
U_{49}	1.5	A_{49}	0.1
U_{56}	4.0	A_{56}	1.0
U_{67}	50.0	A_{67}	1.0
U_{68}	1.5	A_{68}	0.1
U_{69}	1.5	A_{69}	0.1

For the cool-down process, the direct solar irradiation gained by the upper fuselage wall is G_{37} = 1200 W/m^2. Also, considering that the cabin passenger windows are closed results in G_{27} = 0. The outside ambient air temperature is assumed as T_7 = 40^{o}C, representing a summer hot-day ground conditions. A typical air-cycle machine, operating in the cooling process, insufflates air into the aircraft cabin with a temperature T_{in1} = 15^{o}C (ASHRAE, 1999). Initial conditions for a heat-soaked aircraft are assumed equal to: T_1 = 50^{o}C (cabin inside air); T_2 = 50^{o}C (seat); T_3 = 60^{o}C (upper fuselage wall); T_4 = 50^{o}C (floor); T_5 = 50^{o}C (under floor air); T_6 = 50^{o}C (lower fuselage wall).

Figure (4) shows the cool-down time-dependent temperature profiles for each cabin sub-domain. After 2000 s, the cabin inside air temperature is below 25^{o}C which agrees with the certifications requirements and the steady-state value is in the recommended temperature thermal comfort range. The seat temperature also is very important to the passenger thermal comfort conditions. Although its temperature exhibits a delayed profile in comparison with the cabin air, after 2000 s, the seat temperature is lower than the normal passenger body temperature. At this studied case, there is only one heat source that is solar radiation. Upper fuselage wall, that presents highest temperature, absorbs solar energy and supply the other elements through thermal circuit links. Floor shows the slowest temperature response and even after 4000 s the steady-state isn't still attained.

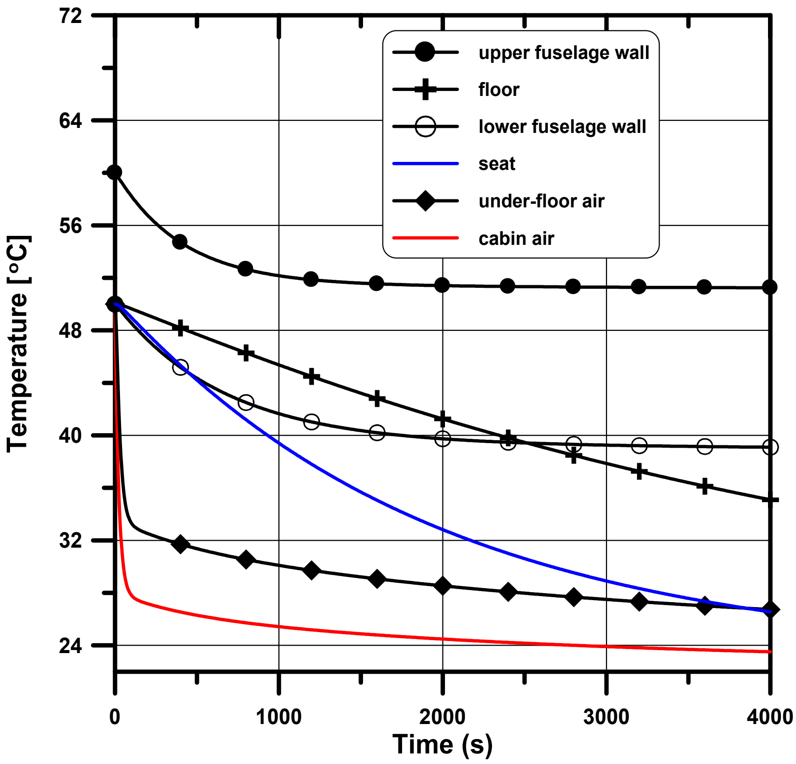

Figure 4. Cool-down temperature profiles.

For the warm-up process, the worst condition implies that the direct solar irradiation G_{37} = G_{27} = 0. The outside ambient air temperature is assumed as T_7 = -20^{o}C, representing a winter cold-day ground conditions. The temperature of the heating air insufflated into the cabin is T_{in1} = 32^{o}C. Initial conditions for a cold-soaked aircraft are assumed equal to: T_1 = -20^{o}C (cabin inside air); T_2 = -20^{o}C (seat); T_3 = -20^{o}C (upper fuselage wall); T_4 = -20^{o}C (floor); T_5 = -20^{o}C (under floor air); T_6 = -20^{o}C (lower fuselage wall). The overall heat transfer coefficients U_{37} and U_{67} take account the radiative heat transfer between the fuselage external surface and the clear night sky.

Figure (5) shows the results for the warm-up time-dependent temperature. Now, the heat source is the heating-air insufflated into the passenger cabin. The cabin inside air shows a steep temperature increase reaching about 20^{o}C after 1500 s. Seat temperature exhibits a smooth response but has the closest value to the steady-state cabin air temperature. Again, the floor temperature shows the slowest time-response. Upper and lower fuselage walls have a similar time-behavior and present the lowest steady-state values due to the absence of solar radiation.

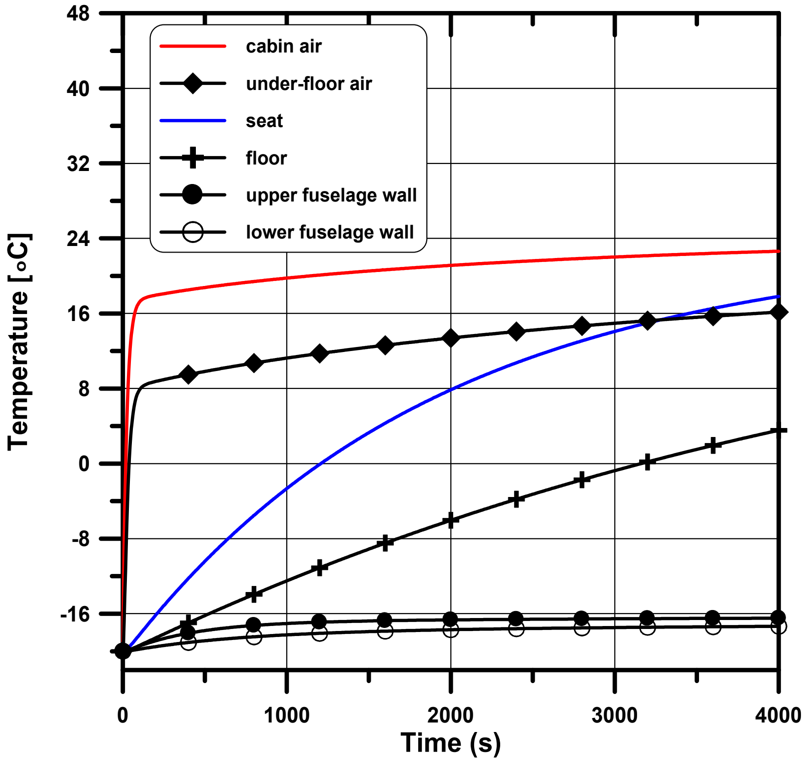

Figure 5. Warm-up temperature profiles.

5. Conclusions

In the present study the unsteady temperatures of the warm-up and cool-down processes for a typical aircraft cabin cross-section were simulated applying the lumped parameter approach with a one-dimensional analog thermal circuit linking the cabin sub-domains. The employed methodology provided physically consistent results and showed that for both cool-down and warm-up processes the passenger thermal comfort conditions (cabin inside-air) are satisfied after less than 2000 s. It was shown that this computational tool can reduce both the design time-consuming and the number of experimental tests to adjust the final environmental control system configuration.

Future studies could include, for example, the effect of a solar radiation space-variable distribution on the fuselage wall time-response.

6. References

American Society of Heating, Refrigerating and Air-Conditioning Engineers, "ASHRAE Handbook, Applications Volume", 1999 , Inc. Atlanta, GA.

Conceição, E. Z. E.; Silva, M. C. G.; André, J. C. S. and Viegas, D. X., 1999, "A Computational Model to Simulate the Thermal Behaviour of the Passengers Compartment of Vehicles", SAE Technical Paper Series, 1999-01-0778.

Ding, Y. and Zito R., 2001, "Cabin Heat Transfer and Air Conditioning Capacity", SAE Technical Paper Series, 2001 01-0284.

Fang, X., 1999, "Mathematical Simulation of Transient Thermal Process of Aircraft Cabins", SAE Technical Paper Series,

Gielda, T.P.; Webster, B.E.; Hesse, M.W.; Calver W. and Halt, D.W., 1996, "The Impact of Computational Fluid Dynamics on Automotive Interior Comfort Engineering", AIAA 34th Aerospace Sciences Meeting and Exhibit, Reno, NV Jan 15-18.

Hoffman, J.D., 1993, "Numerical Methods for Engineers and Scientists", McGraw-Hill, Inc., Singapore.

Huang, D.C., Oker, E., Yang, S.L. and Arici, O., "A Dynamic Computer-Aided Engineering Model For Automotive Climate Control System Simulation and Application Part II: Passenger Compartment Simulation And Applications". SAE Paper 1999-01-1196.

Kasahara, M; Kuzuu, Y.; Matsuba, T.; Hashimoto, Y.; Kamimura, K. and Kurosu, S., 1998, "Physical Model of an Air-Conditioned Space for Control Analysis", ASHRAE Transactions: Research, 304-317.

Kojima, K., Itoh, S., Ohtaki, H. and Watanuki, K., 1999. "An Estimate of Temperature in a Passenger Compartment by Numerical Simulation Using the Linear Graph Theory", SAE Paper 1999-01-1188.